



# Formation and mechanical properties of Ni-free Zr-based bulk metallic glasses

Nengbin Hua, Ran Li, Hui Wang, Jianfeng Wang, Yan Li, Tao Zhang\*

Key Laboratory of Aerospace Materials and Performance (Ministry of Education), School of Materials Science and Engineering, Beihang University, 100191 Beijing, China

## ARTICLE INFO

### Article history:

Received 3 July 2010

Received in revised form

29 December 2010

Accepted 10 January 2011

Available online 21 January 2011

### Keywords:

Bulk metallic glass

Glass-forming ability

Thermal stability

Mechanical properties

## ABSTRACT

Glass formation and mechanical properties of Zr–Al–Co–Cu–Ag bulk metallic glasses (BMGs) were investigated. The glass-forming ability (GFA) of  $Zr_{55}Al_{20}Co_{20}Cu_5$  alloy is significantly improved with minor addition of Ag, indicating by the impressive increase of the critical diameter of glass formation from 5 mm for  $Zr_{55}Al_{20}Co_{20}Cu_5$  to 16 mm for  $(Zr_{0.55}Al_{0.20}Co_{0.20}Cu_{0.05})_{97}Ag_3$  and  $(Zr_{0.55}Al_{0.20}Co_{0.20}Cu_{0.05})_{95}Ag_5$  alloys. The Zr–Al–Co–Cu–Ag BMGs exhibit high compressive strength of 2160–2280 MPa and distinct plasticity of 0.6–2.5%. The Zr-based BMGs with outstanding GFA and mechanical properties as well as low-level cytotoxicity elements are expectative for industrial and biological applications.

© 2011 Elsevier B.V. All rights reserved.

## 1. Introduction

Zr-based bulk metallic glasses (BMGs) are one of the most attractive alloys due to their combinative properties of high glass-forming ability (GFA), superior strength (~2 GPa), high elastic strain limit (~2%), relatively low Young's modulus (80–100 GPa) and excellent corrosion resistance, which make them as good candidates to have promising applications as structural materials and biomaterials [1–5]. Zr–Ti–Ni–Cu–Be [6], Zr–Cu–Ni–Al [7,8] are two classic Zr-based BMG systems with the critical diameter ( $d_c$ ) of more than 10 mm. Moreover, these Zr-based BMGs exhibited a good corrosion resistance in phosphate-buffered saline (PBS) [9,10]. However, in the viewpoint of biocompatibility, these Zr-based BMGs containing highly toxic elements (e.g. Ni, Be or high-concentration Cu) are not suitable for the applications as biomaterials. Therefore, the development of biocompatible Zr-based BMGs without highly toxic element like Be and Ni [11], is required. The efficient efforts have been done in several candidate alloy systems, such as Zr–Al–Cu–Ag [12], Zr–Al–Cu–Fe [13], Zr–Al–Cu–Pd–Nb [14], Zr–Al–Co–Nb [4] and Zr–Al–Co–(Cu) [15,16] so far. Glassy rods with a diameter of at least 15 mm can be obtained in the Zr–Al–Cu–Ag–(Pd) [17,18] and Zr–Al–Fe–Cu [19] system. Recently, glassy rods of  $Zr_{55}Al_{20}Co_{25}$  and near-eutectic  $Zr_{56}Al_{16}Co_{28}$  alloys can be obtained with a diameter of 10 mm and 18 mm, respectively, by using a special method named ladle arc-melting type casting [20]. However, glassy rods of  $Zr_{55}Al_{20}Co_{25}$

alloy only can be produced up to 5 mm in diameter by injection copper mold casting [5].

The Ni-free  $Zr_{55}Al_{20}Co_{20}Cu_5$  alloy exhibited a large supercooled liquid region of 80 K and good mechanical properties, such as large elastic elongation limit of 2.1%, low Young's modulus of 92 GPa and high compressive fracture strength of 2200 MPa, as well as low-level Cu concentration, indicating its good mechanical biocompatibility [16]. However, limited GFA of  $Zr_{55}Al_{20}Co_{20}Cu_5$  alloy ( $d_c = 5$  mm) obstructs the potential application. It has been found that the addition of Ag into Zr-based glassy alloys can improve the GFA, mechanical properties and corrosion resistance [12,21–24]. In this study, the influence of Ag addition (up to 7 at.%) in  $Zr_{55}Al_{20}Co_{20}Cu_5$  precursor alloy on GFA, thermal stability and mechanical properties was investigated. The proper Ag addition of 3–5 at.% can improve the GFA of the resulting alloys indicated by the fully amorphous rods in diameter of up to 16 mm. The compressive mechanical properties were also evaluated in detail. All of the results provide the foundational information of this family of Ni-free Zr-based BMGs for further biological applications.

## 2. Experimental

A series of  $(Zr_{0.55}Al_{0.20}Co_{0.20}Cu_{0.05})_{100-x}Ag_x$  ( $x = 0, 1, 3, 5, 7$  at.%) alloys were prepared by arc melting mixtures of pure Zr, Al, Co, Cu and Ag elements with nominal chemical compositions in Ti-gettered high purity argon atmosphere. Cylindrical samples with a diameter of less than 10 mm were prepared by a Cu-mold injection casting method. For specimens of 10 mm in diameter or larger size, the ingots were remelted in a quartz crucible using an electromagnetic induction heating device and then poured into a copper mold with 50-mm long rod-shaped cavity in a highly pure argon atmosphere. Ribbon samples with a cross section of 0.02 mm × 1.2 mm were also prepared by melt spinning. The structure of the rapidly solidified ribbons and the rod specimens was examined using X-ray diffractometer (XRD, Bruker AXS D8) with  $Cu-K\alpha$  radiation and high-resolution transmission electron micro-

\* Corresponding author.

E-mail address: [zhangtao@buaa.edu.cn](mailto:zhangtao@buaa.edu.cn) (T. Zhang).

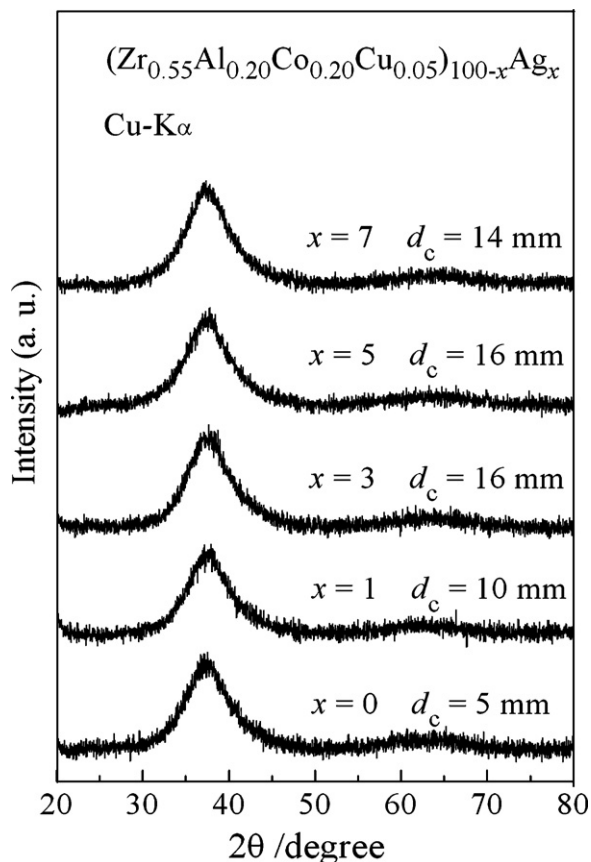


Fig. 1. XRD patterns of as-cast  $(\text{Zr}_{0.55}\text{Al}_{0.20}\text{Co}_{0.20}\text{Cu}_{0.05})_{100-x}\text{Ag}_x$  ( $x=0, 1, 3, 5, 7$  at.%) rods with the critical diameters.

scope (HRTEM, JEM2100F), respectively. The thermal stability associated with glass transition, supercooled liquid and crystallization and the melting behavior for the glassy alloys was investigated by differential scanning calorimetry (DSC, NETZSCH DSC 404 C) at a heating rate of  $0.33 \text{ K s}^{-1}$ . The specimens for the DSC and XRD measurement of the bulk samples were taken from their central part of the cross section. The rod specimens with a diameter of 3 mm and an aspect ratio (height/diameter) of 2 were tested in a compressive condition using a testing machine (CMT5504 SANS, China) at an initial strain rate of  $2.1 \times 10^{-4} \text{ s}^{-1}$  at room temperature. The rod specimens used for compression test were cut from as cast rods with a diameter of 3 mm and a length of 40 mm.

### 3. Results and discussion

Fig. 1 shows XRD patterns of as-cast  $(\text{Zr}_{0.55}\text{Al}_{0.20}\text{Co}_{0.20}\text{Cu}_{0.05})_{100-x}\text{Ag}_x$  ( $x=0, 1, 3, 5, 7$  at.%) rods to indicate their GFA. The patterns of all alloys show one main broad diffraction halo indicating fully glassy structure within the sensitivity limits of X-ray diffraction. The  $d_c$  of  $\text{Zr}_{55}\text{Al}_{20}\text{Co}_{20}\text{Cu}_5$  alloy was 5 mm. After a minor addition of Ag in this precursor alloy, the GFA of the resulting alloys is increased significantly and the  $d_c$  of the glassy rods can be increased to 16 mm for both of  $(\text{Zr}_{0.55}\text{Al}_{0.20}\text{Co}_{0.20}\text{Cu}_{0.05})_{97}\text{Ag}_3$  and  $(\text{Zr}_{0.55}\text{Al}_{0.20}\text{Co}_{0.20}\text{Cu}_{0.05})_{95}\text{Ag}_5$  alloys. Further increase of Ag content up to 7 at.% will deteriorate the GFA. The similar results of the existence of optimized addition concentration have also been reported in other glassy systems, such as  $(\text{Cu}-\text{Zr}-\text{Al})-\text{Ln}$  and  $(\text{Zr}-\text{Al}-\text{Ni}-\text{Cu})-\text{Ln}$ , which can be attributed to the complication of crystallization [2,25,26]. Fig. 2 shows the comparison of DSC curves between as-cast 16-mm rod and as-spun glassy ribbon with the same composition of  $(\text{Zr}_{0.55}\text{Al}_{0.20}\text{Co}_{0.20}\text{Cu}_{0.05})_{95}\text{Ag}_5$ . No appreciable difference in the glass transition temperature ( $T_g$ ), the onset temperature of crystallization ( $T_x$ ) and the heat release of crystallization can be found between the rod and the ribbon. The bright-field TEM

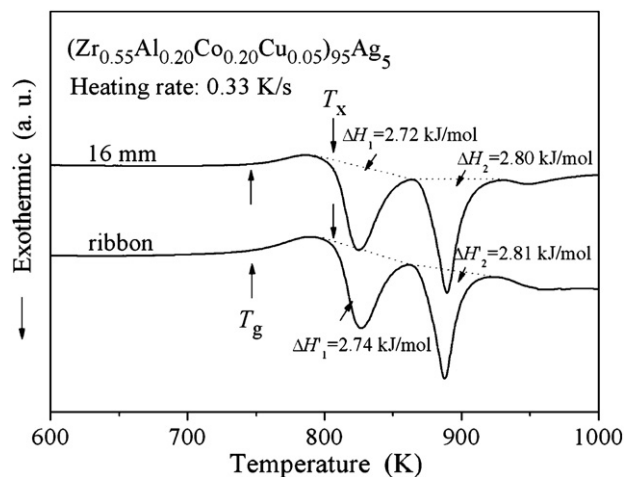


Fig. 2. The comparison of DSC curves between glassy ribbon and as-cast rod of 16 mm in diameter (central region) for  $(\text{Zr}_{0.55}\text{Al}_{0.20}\text{Co}_{0.20}\text{Cu}_{0.05})_{95}\text{Ag}_5$  alloy.

image and selected area electron diffraction (SAED) pattern of  $(\text{Zr}_{0.55}\text{Al}_{0.20}\text{Co}_{0.20}\text{Cu}_{0.05})_{95}\text{Ag}_5$  rod of 16 mm in diameter are shown in Fig. 3. The homogeneous contrast in the images and a broad halo in the SAED pattern indicate that the structure of 16-mm-diameter  $(\text{Zr}_{0.55}\text{Al}_{0.20}\text{Co}_{0.20}\text{Cu}_{0.05})_{95}\text{Ag}_5$  sample is a single amorphous phase.

Fig. 4(a) and (b) shows the glass transition, crystallization and melting behaviors of the  $(\text{Zr}_{0.55}\text{Al}_{0.20}\text{Co}_{0.20}\text{Cu}_{0.05})_{100-x}\text{Ag}_x$  ( $x=0, 1, 3, 5, 7$  at.%) glassy samples. The glass transition temperature ( $T_g$ ), onset temperature of crystallization ( $T_x$ ), melting temperature ( $T_m$ ), and liquidus temperature ( $T_l$ ) are marked by arrows in Fig. 4(a) and (b) and summarized in Table 1. The samples exhibit a clear endothermic heat event characteristic of the glass transition to supercooled liquid, followed by characteristic exothermic transformations corresponding to crystallization of the supercooled liquid. It is found that  $T_g$  increases monotonously from 737 to 753 K with the increase of Ag content, while  $T_x$  decreases from 815 to 806 K.

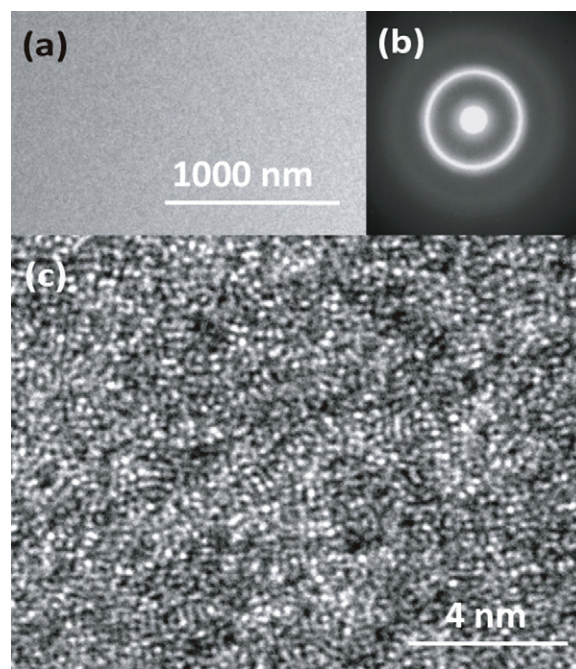
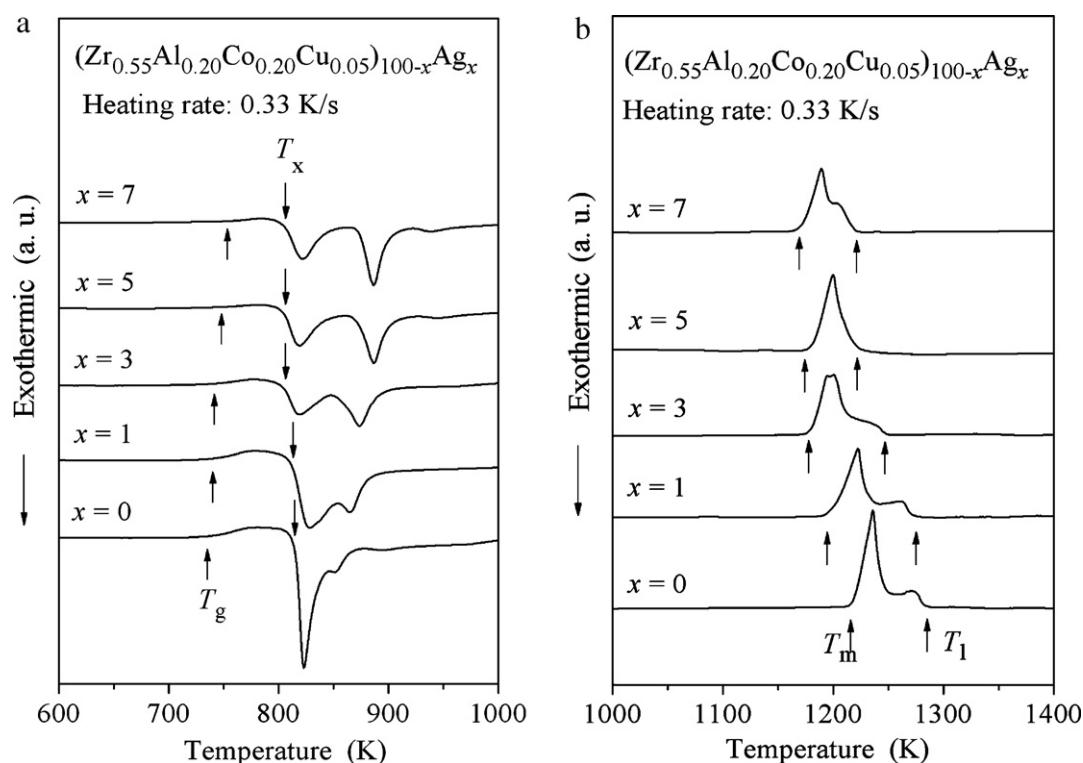


Fig. 3. (a) TEM bright-field image, (b) selected area electron diffraction (SAED) pattern and (c) high-resolution TEM image of the  $(\text{Zr}_{0.55}\text{Al}_{0.20}\text{Co}_{0.20}\text{Cu}_{0.05})_{95}\text{Ag}_5$  glassy rod of 16 mm in diameter. The sample was taken from the center part of the as-cast rod.



**Fig. 4.** (a) DSC curves of  $(\text{Zr}_{0.55}\text{Al}_{0.20}\text{Co}_{0.20}\text{Cu}_{0.05})_{100-x}\text{Ag}_x$  ( $x=0, 1, 3, 5, 7$  at.%) glassy samples in the temperature range of (a) crystallization and (b) melting behaviors at a heating rate of 0.33 K/s.

It results in the decrease of the supercooled liquid region from 78 K to 53 K. Fig. 4(b) shows that the introduction of Ag significantly depresses both of the  $T_m$  and  $T_1$  of the resulting alloys. The  $(\text{Zr}_{0.55}\text{Al}_{0.20}\text{Co}_{0.20}\text{Cu}_{0.05})_{95}\text{Ag}_5$  alloy shows a melting behavior of near-eutectic composition with the lowest  $T_1$  in these alloys, indicating the addition of Ag can promote the formation of an eutectic composition.  $T_g/T_m$ ,  $T_g/T_1$ ,  $\Delta T_x$  ( $\Delta T_x = T_x - T_g$ ) and  $\gamma$  ( $\gamma = T_x/(T_g + T_1)$ ) are usually used as indicators of GFA [27–29]. These parameters of the present alloys are listed in Table 1. It is found that the increase in the Ag addition content results in the increase in  $T_{rg}$  and  $\gamma$  values, which can give a good explanation of the enhancement of GFA. On the other hand, the supercooled liquid region decreases from 78 K to 53 K with increasing Ag content, which is not in consistency with the change in GFA of the Zr–Al–Co–Cu–Ag alloys [27].

Previous studies showed that atomic-size mismatch and efficient atomic packing may enhance GFA of a system [27]. In the Zr–Al–Co–Cu–Ag system, the atomic radius of Zr, Al, Co, Cu, and Ag are 0.158 nm, 0.143 nm, 0.125 nm, 0.128 nm, and 0.144 nm, respectively [27]. The atomic radius of Ag is significantly different from that of component elements of Zr, Co and Cu, while the difference between Ag and Al is slight. The proper adjustment of atomic size mismatch by the introduction of Ag may result in a more efficiently packed local structure, leading to a superior GFA [27]. In addition, the heats of mixing for Zr–Ag and Al–Ag pairs are  $-20$  and  $-4$  kJ/mol, respectively, while the ones of Co–Ag pair and Cu–Ag pair are 19 kJ/mol and 2 kJ/mol, respectively [30]. The proper adjust-

ment of the heats of mixing associated with the concentration between Ag and the other component elements would improve the stability of local cluster and restrain long-range diffusion of atoms in liquid, thus enhancing the GFA [25]. High content of Ag addition in the Zr–Al–Co–Cu alloy would result in segregation of the component atoms and increase the potential energy of a system [31]. Therefore, as the  $x$  is increased over 5 at.%, the GFA begins to deteriorate.

Fig. 5 shows compressive stress–strain curves of  $(\text{Zr}_{0.55}\text{Al}_{0.20}\text{Co}_{0.20}\text{Cu}_{0.05})_{100-x}\text{Ag}_x$  ( $x=0, 1, 3, 5, 7$  at.%) glassy rods. The yield strength ( $\sigma_y$ ), compressive strength ( $\sigma_c$ ) and plastic strain ( $\epsilon_p$ ) were listed in Table 1. The yield strength is determined by the crossover point from elastic to plastic portions with a very small offset of 0.05%. The stress–strain curves are characteristic of an elastic limit of  $\sim 2\%$  for BMGs, followed by yielding and a serrated plastic deformation before fracture failure. This family of Zr–Al–Co–Cu–Ag BMGs exhibits high compressive strength values of  $\sim 2.2$  GPa, which is higher than that of other Zr-based alloy such as Zr–Al–Ni–Cu, Zr–(Ti–Nb–Pd)–Al–Ni–Cu, Zr–Ti–Ni–Cu–Be [16], a Young's modulus of 98–102 GPa, and a distinct plasticity of 0.6–2.5%. The addition of Ag will not significantly depress the strength and plasticity in this Zr–Al–Co–Cu–Ag system. This family of Ni-free Zr-based BMGs with high GFA and good mechanical properties is expected to have wide applications as biomaterials. More studies about the biocompatibility and corrosion behaviors of the Zr–Al–Co–Cu–Ag BMGs are in progress.

**Table 1**

Glass formation, thermal properties and mechanical properties of  $(\text{Zr}_{0.55}\text{Al}_{0.20}\text{Co}_{0.20}\text{Cu}_{0.05})_{100-x}\text{Ag}_x$  ( $x=0, 1, 3, 5, 7$  at.%) glassy alloys.

Ag content	$d_c$ /mm	$T_g$ /K	$T_x$ /K	$T_m$ /K	$T_1$ /K	$\Delta T_x$ /K	$\gamma$	$T_g/T_m$	$T_g/T_1$	$\sigma_y$ /MPa	$\sigma_c$ /MPa	$\epsilon_p$ (%)	$E$ /GPa
$x=0$	5	737	815	1215	1285	78	0.403	0.61	0.57	2080	2160	1.3%	102
$x=1$	10	739	813	1194	1275	74	0.404	0.62	0.58	2080	2180	2.5%	102
$x=3$	16	740	805	1178	1246	65	0.405	0.63	0.59	2010	2210	1.4%	98
$x=5$	16	747	806	1174	1220	59	0.410	0.64	0.61	2000	2170	1%	98
$x=7$	14	753	806	1169	1222	53	0.408	0.64	0.62	2100	2280	0.6%	100

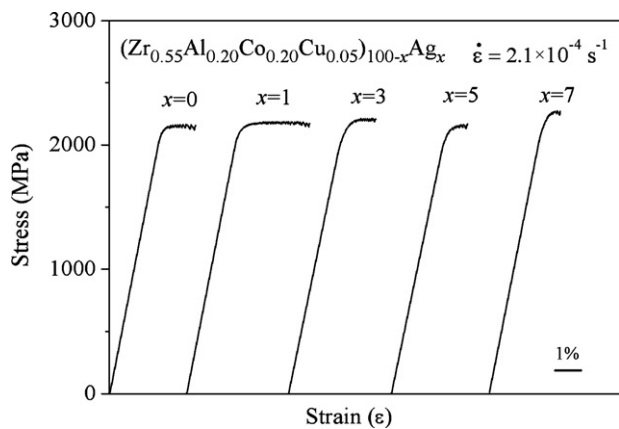


Fig. 5. Compression stress–strain curves of  $(\text{Zr}_{0.55}\text{Al}_{0.20}\text{Co}_{0.20}\text{Cu}_{0.05})_{100-x}\text{Ag}_x$  ( $x=0, 1, 3, 5, 7$  at.%) glassy rods of 3 mm in diameter.

#### 4. Conclusions

The addition of Ag can significantly improve the GFA of Zr–Al–Co–Cu system and a series of centimeter-size Zr–Al–Co–Cu–Ag BMGs can be synthesized by copper mold casting. The glassy rods of 16 mm in diameter were obtained for the  $(\text{Zr}_{0.55}\text{Al}_{0.20}\text{Co}_{0.20}\text{Cu}_{0.05})_{97}\text{Ag}_3$  and  $(\text{Zr}_{0.55}\text{Al}_{0.20}\text{Co}_{0.20}\text{Cu}_{0.05})_{95}\text{Ag}_5$  alloys. The high  $T_{\text{rg}}$  and  $\gamma$  values are responsible for high GFA of Zr–Al–Co–Cu–Ag BMGs. The Ni-free Zr–Al–Co–Cu–Ag BMGs with high GFA exhibit good mechanical properties with high compressive strength of 2.2 GPa as well as distinct plasticity of 0.6–2.5%, which makes them as promising materials for industrial and bio-applications.

#### Acknowledgements

This work was financially supported by the National Basic Research Program of China (2007CB613900), the National Nature

Science Foundation of China (Grant Nos. 50631010, 50771005, 51071008, and 50771006) and Program for New Century Excellent Talents in University (NCET-07-0041).

#### References

- [1] W.L. Johnson, MRS Bull. 24 (1999) 42–56.
- [2] W.H. Wang, C. Dong, C.H. Shek, Mater. Sci. Eng. R 44 (2004) 45–89.
- [3] A.L. Greer, E. Ma, MRS Bull. 32 (2007) 611–619.
- [4] S.J. Pang, T. Zhang, K. Asami, A. Inoue, J. Mater. Res. 18 (2003) 1652–1658.
- [5] Q.K. Jiang, X.P. Nie, Y.G. Li, Y. Jin, Z.Y. Chang, X.M. Huang, J.Z. Jiang, J. Alloys Compd. 443 (2007) 191–194.
- [6] A. Peker, W.L. Johnson, Appl. Phys. Lett. 63 (1993) 2342.
- [7] A. Inoue, T. Zhang, N. Nishiyama, K. Ohba, T. Masumoto, Mater. Trans. JIM 34 (1993) 1234–1237.
- [8] A. Inoue, T. Zhang, Mater. Trans. JIM 37 (1996) 185–187.
- [9] M.L. Morrison, R.A. Buchanan, R.V. Leon, C.T. Liu, B.A. Green, P.K. Liaw, J.A. Horton, J. Biomed. Mater. Res. A 74A (2005) 430–438.
- [10] S. Hiromoto, A.-P. Tsai, M. Sumita, T. Hanawa, Corros. Sci. 42 (2000) 1651–1660.
- [11] A. Yamamoto, R. Honma, M. Sumita, J. Biomed. Mater. Res. 39 (1998) 331–340.
- [12] W. Zhang, Q.S. Zhang, C.L. Qin, A. Inoue, Mater. Sci. Eng. B 148 (2008) 92–96.
- [13] K. Jin, J.F. Löffler, Appl. Phys. Lett. 86 (2005) 241909.
- [14] C.L. Qiu, Q. Chen, L. Liu, K.C. Chan, J.X. Zhou, P.P. Chen, S.M. Zhang, Scripta Mater. 55 (2006) 605–608.
- [15] T. Wada, T. Zhang, A. Inoue, Mater. Trans. JIM 43 (2002) 2843–2846.
- [16] T. Wada, T. Zhang, A. Inoue, Mater. Trans. JIM 44 (2003) 1839–1844.
- [17] Q.K. Jiang, X.D. Wang, X.P. Nie, G.D. Zhang, H. Ma, H.J. Fecht, J. Bendnar-cik, H. Franz, Y.G. Liu, Q.P. Cao, J.Z. Jiang, Acta Mater. 56 (2008) 1785–1796.
- [18] Q.S. Zhang, W. Zhang, A. Inoue, Mater. Trans. JIM 48 (2007) 3031–3033.
- [19] Q.S. Zhang, W. Zhang, A. Inoue, Scripta Mater. 61 (2009) 241–244.
- [20] T. Wada, F.X. Qin, X.M. Wang, M. Yoshimura, A. Inoue, N. Sugiyama, R. Ito, N. Matsushita, J. Mater. Res. 24 (2009) 2941–2948.
- [21] W. Zhang, F. Jia, Q.S. Zhang, A. Inoue, Mater. Sci. Eng. A 459 (2007) 330–336.
- [22] D.S. Sung, O.J. Kwon, E. Fleury, K.B. Kim, J.C. Lee, D.H. Kim, Y.C. Kim, Met. Mater. Int. 10 (2004) 575–579.
- [23] Z. Liu, K.C. Chan, L. Liu, J. Alloys Compd. 487 (2009) 152–156.
- [24] C. Zhang, N. Li, J. Pan, S.F. Guo, M. Zhang, L. Liu, J. Alloys Compd. 504S (2010) S163–S167.
- [25] D.H. Xu, G. Duan, W.L. Johnson, Phys. Rev. Lett. 92 (2004) 245504.
- [26] J. Luo, H.P. Duan, C.L. Ma, S.J. Pang, T. Zhang, Mater. Trans. 47 (2006) 450–453.
- [27] A. Inoue, Acta Mater. 48 (2000) 279–306.
- [28] D. Turnbull, Contemp. Phys. 10 (1969) 473–488.
- [29] Z.P. Lu, C.T. Liu, Acta Mater. 50 (2002) 3501–3512.
- [30] A. Takeuchi, A. Inoue, Mater. Trans. 46 (2005) 2817–2829.
- [31] J.H. He, H.W. Sheng, E. Ma, Appl. Phys. Lett. 78 (2001) 1343–1345.